J. Phycol. **45,** 119–129 (2009)

DOI: 10.1111/j.1529-8817.2008.00616.x

RESPONSES TO SOLAR UV RADIATION OF THE DIATOM *SKELETONEMA COSTATUM* (BACILLARIOPHYCEAE) GROWN AT DIFFERENT Zn^{2+} CONCENTRATIONS[1]

Guang Gao, Kunshan Gao[2]

State Key Laboratory of Marine Environmental Science, Xiamen University, Xiamen, 361005, China

and Mario Giordano

Department of Marine Sciences, Università Politecnica delle Marche, 60131 Ancona, Italy

Zn availability in the ocean has been suggested to limit primary production by affecting CO_2 acquisition processes for photosynthesis, therefore influencing the global carbon cycle. Also, UV radiation (UVR, 280–400 nm) is known to affect primary production in different ways. It remains to be ascertained whether Zn availability and UVR can act synergistically, antagonistically, or independently on oceanic primary production. We cultured the cosmopolitan diatom *Skeletonema costatum* (Grev.) Cleve under different radiation treatments with or without UVR (only photosynthetically active radiation), at 0, 3, and 10 pmol · L^{-1} Zn^{2+}. Specific growth rate, photosynthetic carbon assimilation, external carbonic anhydrase (eCA) activity, and estimated cell abundance increased with increasing concentrations of Zn^{2+} from 0 to 3 and 10 pmol · L^{-1}, irrespective of the radiation treatment. Higher eCA activity was observed in the cells grown at the high level of Zn^{2+} in the presence of UVR. An approximately linear relationship between μ and the daily dose of PAR was observed at 3 and 10 pmol · L^{-1} Zn^{2+} concentrations. However, the dependency of μ on the daily PAR dose disappeared when the cells were grown in the presence of UVR, which overall depressed both μ and photosynthetic carbon assimilation. The inhibitory effect of UVR was inversely related to Zn^{2+} concentrations. The ultraviolet-B (UVB)-related inhibition of growth and photosynthesis decreased with time, reflecting a faster acclimation of the cells to UVR at replete Zn^{2+} levels. Overall, growth in the presence of higher Zn^{2+} concentrations reduced the sensitivity to UV radiation in *Skeletonema costatum*.

Key index words: **carbonic anhydrase; growth; inhibition; photosynthesis; *Skeletonema costatum*; UV radiation; Zn limitation**

Abbreviations: **CA, carbonic anhydrase; eCA, external carbonic anhydrase; PA, PAR + UVA; PAB, PAR + UVA + UVB; UVA, ultraviolet radiation A; UVB, ultraviolet radiation B; UVR, ultraviolet radiation**

More than 98% of Zn in oceanic surface seawater is organically complexed (Bruland 1989), leading to concentrations of free Zn^{2+} in the nanomolar range (Ellwood and Van den Berg 2000, Franck et al. 2003) and often lower than a few picomoles per liter (Bruland 1989, Bruland et al. 1991). The optimum Zn^{2+} concentration for marine microalgal growth is often higher than even the highest of these values (Buitenhuis et al. 2003, Hu et al. 2003). Of the nearly 300 enzymes that use Zn^{2+} as a metal cofactor (Vallee and Auld 1990), carbonic anhydrase (CA) is one of the most abundant in marine microalgae (Tobin 1970, Sunda and Huntsman 1992, Morel et al. 1994). Zn availability may therefore impact on primary production by influencing the CO_2-acquisition processes in which CA is involved (Morel et al. 1994, Buitenhuis et al. 2003, Giordano et al. 2005).

Solar UVR can cause a decline in algal photosynthesis (Schofield et al. 1995, Nilawati et al. 1997, Helbling et al. 2003) and growth (Nilawati et al. 1997, West et al. 1999, Xenopoulos et al. 2002, Villafañe et al. 2003) and can affect the activity of enzymes, such as RUBISCO (Bischof et al. 2002). However, UVR has also been shown to act positively, triggering signaling responses (Brunner et al. 2000, Lin 2002, Huang et al. 2004), inducing repair of damaged DNA (Karentz et al. 1991), and enhancing photosynthetic carbon fixation under fast mixing or reduced levels of solar radiation (Barbieri et al. 2002, Helbling et al. 2003, Gao et al. 2007).

Marine diatoms are responsible for ~40% of oceanic primary productivity (Nelson et al. 1995). In marine environments, dissolved inorganic carbon (DIC, ~2 mM) is present in the forms of CO_2, HCO_3^-, and CO_3^{2-}, with HCO_3^- accounting for >90% and CO_2 usually <1%. The concentration of CO_2 for saturating half of the RUBISCO activity (K_m) is ~30–60 μmol · L^{-1} (Badger et al. 1998), which is much higher than the availability of CO_2 in

[1]Received 11 November 2007. Accepted 25 July 2008.
[2]Author for correspondence: e-mail ksgao@xmu.edu.cn.

natural seawater (~10 μmol · L^{-1} at 15°C, pH 8.2, salinity 35‰). To maintain efficient photosynthesis, many phytoplankton species have developed carbon-concentrating mechanisms (CCMs), which raise the CO_2 concentration around the active site of RUBISCO (Raven and Falkowski 1999, Raven and Beardall 2003). *S. costatum,* a cosmopolitan and ecologically relevant marine diatom, is known to be able to induce a CCM in response to a reduction of CO_2 availability (Nimer et al. 1998, Rost et al. 2006). In spite of this, *S. costatum* showed reduced growth when there was not enough light energy to drive a CCM, and enrichment of CO_2 enhanced its growth at both light- and CO_2-limited conditions (Chen and Gao 2003). Extracellular carbonic anhydrase (eCA) is allegedly a component of the CCM of this species (Nimer et al. 1998, Chen and Gao 2004), and it has been reported that Zn^{2+} availability affects CA activity in diatoms (Morel et al. 1994, Hu et al. 2003, Shi et al. 2004). *S. costatum* is therefore an excellent experimental organism to test the hypothesis that Zn availability affects photosynthesis and growth via inorganic C acquisition.

Most experiments on Zn-related effects have been conducted under artificial illumination, with undetermined levels or absence of UVR. To achieve a better understanding of the effect of Zn availability on growth, photosynthesis, and CA activity, under natural solar radiation, we designed and conducted experiments on *S. costatum* cultured in the presence of different Zn^{2+} concentrations and concomitantly exposed to natural daily fluctuations in light with or without UVR.

MATERIALS AND METHODS

Organism and growth conditions. *S. costatum* strain 2042 was obtained from the Ocean University of China. The cells had been cultured in artificial seawater (Harrison et al. 1980) with the modified f/2 medium without Zn, Cd, or Co. Since Zn^{2+} has been reported to be ~2 pM in the surface seawater of the central North Pacific (Bruland et al. 1991), 6–20 pM in the northeastern Atlantic Ocean (Ellwood and Van den Berg 2000), and 1–10 pM in North Pacific surface waters (Brand et al. 1983, Sunda and Huntsman 1992), the levels of 0, 3, 10 pmol · L^{-1} Zn^{2+} were set up to reflect natural Zn^{2+} concentrations in the ocean. EDTA was added at a concentration of 100 μM to buffer free ion concentration of Zn^{2+}. Different Zn^{2+} concentrations were obtained by adding appropriate amounts of $ZnCl_2$ to the Zn-free medium (Sunda and Huntsman 1995). The experimental vessels were soaked in 1 mol · L^{-1} HCl overnight and carefully rinsed with distilled water before use. Initially, cells were allowed to grow for six generations in the presence of 3 pmol · L^{-1} Zn^{2+} (the Zn^{2+} concentration in f/2 medium), in a growth cabinet (model 515; White Westinghouse, Pittsburgh, PA, USA), at 22°C. During this phase, light was provided by cool-white fluorescent light (PAR), at a photon flux density of 90 μmol photons · m^{-2} · s^{-1} (12:12 light:dark [L:D]). Subsequently, cells in the exponential growth phase acclimated to the conditions described above were harvested by centrifugation (5804R; Eppendorf, Hamburg, Germany; 6,000*g,* 15 min, 20°C), washed twice with fresh medium, and resuspended in the medium of designed Zn^{2+} concentration, at a cell density of 1.6×10^5 cells · mL^{-1}. These cultures were immediately subjected to the selected radiation treatment (see next section) and grown semicontinuously. Cell concentration was monitored every day at 5:30 p.m. Dilution with fresh medium was effected every 24 h to reestablish the initial cell density (1.6×10^5 cells · mL^{-1}). All cultures were bubbled with a flow of 1 L · min^{-1} with filtered (PTFE 0.2 μm; Whatman, Maidstone, UK) ambient air. Another 0.2 μm gas filter was placed on the gas outlet line.

Radiation measurement and treatment. Incident solar radiation was continuously monitored using a broadband filter radiometer (ELDONET; Real Time Computer Inc., Erlangen, Germany) with three channels for UVB (280–315 nm), UVA (315–400 nm), and PAR (400–700 nm). The radiometer, located on a roof of Shantou University (23.3° N, 116.6° E), measured the irradiances every second and recorded the means for every minute (Häder et al. 1999, Korbee-Peinado et al. 2004). The reliability of this instrument has been internationally recognized (Häder et al. 1999, Korbee-Peinado et al. 2004) and certified with the correspondence error lower than 0.5% in comparison with the most accurate instrument (certificate No. 2006/BB14/1).

The cultures were maintained in quartz tubes (16 cm in length and 5.5 cm inner diameter) in a thermostatic water bath (20 ± 1°C). The following radiation treatments were imposed on the cultures (triplicates for each treatment):

(1) PAR; for this treatment the quartz tubes were covered with Ultraphan UV Opak cut-off foil (Digefra, Munich, Germany), transmitting wavelength above 395 nm.

(2) PAR + UVA (PA); to attain this condition, the quartz tubes were covered with 320 nm cut-off foil (Montagefolie, Folex, Dreieich, Germany). There was a 5 nm difference between the measured and exposed UVA irradiance, which gives ~2% higher percent of UVA than that the cells were actually exposed to.

(3) PAR + UVA + UVB (PAB); in this case, the quartz tubes were covered with Ultraphan cut-off foil (Digefra, Munich, Germany), that transmits radiations above 295 nm. Also, these tubes were covered with foil to ensure that the same PAR reflection (4%) as for the other radiation treatments (Gao et al. 2007). No cut-off filters significantly affected light quality in the PAR region, and their transmission spectra have been reported elsewhere (Korbee-Peinado et al. 2004).

Measurements of cell growth and pigment concentrations. Cell concentration was determined every day at 5:30 p.m. by direct counting with an improved Neubauer haemocytometer (XB-K-25; Qiu Jing, Shanghai, China). All counts were carried out in three replicates. Specific growth rate (μ) was determined from the changes in the cell concentration over 24 h as:

$$\mu = \ln(C_n/C_{n-1})(t_n - t_{n-1})^{-1} \quad (1)$$

where C_n and C_{n-1} represent the cell concentrations at time t_n and t_{n-1}, respectively.

To determine the chl *a* content, 45 mL of culture was filtered on a Whatman GF/F filter, extracted in 5 mL of absolute methanol overnight at 4°C, centrifuged (2,000*g,* 10 min), and the optical density of the supernatant was scanned from 250 to 750 nm with a UV-VIS spectrophotometer (Shimadzu UV-1206; Kyoto, Japan). The concentration of chl *a* was calculated using the equation of Porra (2002), and that of carotenoid was estimated according to Parsons and Strickland (1963). The peak areas of the absorption spectra in the UV regions (260–300 nm) were integrated using Origin software (7.0, Originlab Corp., Northhamption, MA, USA) to estimate approximately the abundances of these pigments.

Measurement of photosynthetic carbon fixation rate. The cells cultured as described above were sampled at 1:30 p.m. An aliquot of the culture was filtered through a Whatman GF/F filter. The concentration of the dissolved inorganic carbon (DIC) in the medium was determined using a TOC analyzer (TOC-5000A Shimadzu), which determines DIC by automatically acidifying the seawater and measuring the released CO_2. A 15 mL aliquot of the same culture was placed in quartz tubes (6.9 cm long and 1.7 cm in inner diameter). A volume of 0.1 mL of 2 μCi (0.074 MBq) of ^{14}C-labeled sodium bicarbonate (Amersham, Buckinghamshire, England) was added to each tube. The tubes were then immediately exposed to the same radiation regime used for growth for 2 h. The ^{14}C incorporated via photosynthesis was determined with a liquid scintillation counter (LS 6500, Beckman Coulter, Fullerton, CA, USA), and the carbon fixation rate was obtained as described by Holm-Hansen and Helbling (1995).

Determination of external carbonic anhydrase activity. External carbonic anhydrase (eCA) was determined potentiometrically following the method of Wilbur and Anderson (1948). Cells were centrifuged at 5,000*g*, washed once with 20 mM Na-barbital buffer (pH 8.2), and resuspended in 4 mL of the same buffer. CO_2-saturated distilled water (2 mL) was gently injected into the cell suspension (containing 20 mmol · L^{-1} Veronal buffer, 1.6×10^7 cells · mL^{-1}), and the time required for the pH to decrease at 4°C from pH 8.2 to 7.2 was recorded. CA activity was calculated using the following formula: E.U. = 10 * (T_0/T–1), where T_0 and T represent the time required for the pH change in the absence or presence of the cells, respectively. The measurement of the eCA activity was carried out on days 4 and 10, 1 d in advance of the measurement of photosynthetic carbon fixation.

To convert the potentiometric measurements in actual catalytic rates and to estimate CA abundance, we applied the procedure described by Ratti et al. (2007). On the basis of the genome data available for diatoms (http://genome.jgi-psf.org/), it was assumed that the external CA of *Skeletonema* was an α-type CA. Since no information is available on the kinetic constants of diatoms or algal eCA in the dehydration direction, the constants used for the calculations were derived from other α-CA, for which catalytic constants were available. The constants used were: $K\text{cat}^{HCO_3^-} = 3.66 \times 10^5$ s^{-1}, $K_M{}^{HCO_3^-} = 47$ mM from human erythrocytes ''type-C'' CA, all determined at 20°C (Sanyal and Maren 1981). As a check, the same calculations were also performed with the constants given by Ratti et al. (2007).

Statistical methods. Statistical significance of differences was determined with *t*-test or one-way analysis of variance (ANOVA), with the significant level set at 0.05, unless otherwise indicated.

RESULTS

Daily doses of PAR, UVA, and UVB. The daily doses of PAR, UVA, and UVB radiation over the course of the experiment (11 d) are presented in Figure 1A. The mean daily doses of PAR, UVA, and UVB over this period were 5.24, 0.85, and 0.020 MJ · m^{-2}, respectively. The solar PAR dose was ~4.34 MJ · m^{-2} on day 1, rose to 6.82 MJ · m^{-2} on day 2, which was characterized by a clear sky, and then continuously declined to 2.92 MJ · m^{-2} all the way to day 6, due to overcast conditions. Two consecutive days with higher levels of radiation followed. The last 3 d were sunny days with radiation levels similar to that on day 2.

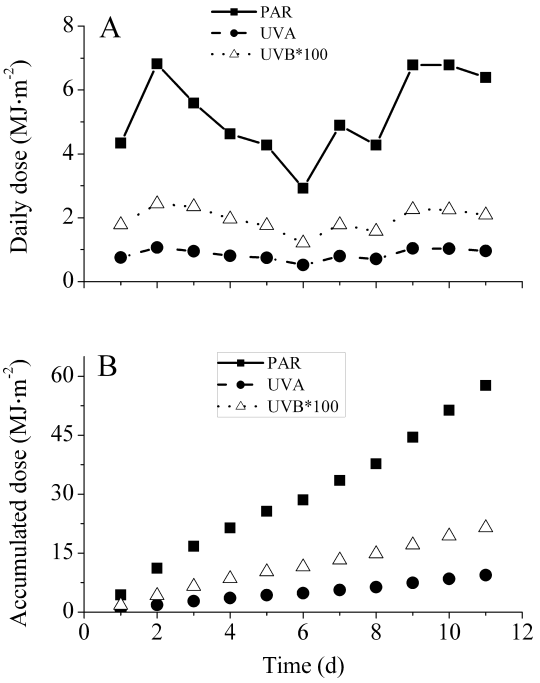

FIG. 1. Daily doses (A) and accumulated doses (B) of PAR, UVA, and UVB during the experiment (11 d).

Panel B in Figure 1 shows the incremental doses of PAR, UVA, and UVB to which cells were subjected on each day. It can be seen that the rate of increase of accumulated radiation is substantially higher for PAR than for UVA and UVB, with a rate of UVB radiation accumulation that is slightly higher than that of UVA.

Effect of the presence of UVA and/or UVB on growth, in the presence of different Zn^{2+} concentrations. Cells showed higher specific growth rates (μ) under PAR than under PAB, on most of the days except days 1, 6, and 8, when solar radiation was lowest (Fig. 2, A–C). The growth rate in the presence of PA was lower than that under PAR alone, on the sunny days (days 2, 9, 10). The only sunny day in which growth rate was higher under PAR was day 11; however, on the cloudy days, the growth rates of cultures exposed to PA was higher than (days 1, 4, 7—at 3 and 10 pmol Zn^{2+} · L^{-1}) or equal to (days 3, 5, 6—at 0 pmol Zn^{2+} · L^{-1}) that measured under the PAR treatment (Fig. 2, A–C). It is also noteworthy that, on the days on which growth under PA was higher than that under PAR, the difference between the growth rates under the two radiation treatments was larger when the medium contained more Zn^{2+} (Fig. 2, B and C).

Over the experimental time period, the specific growth rate of *S. costatum* in the presence of 3 pmol Zn^{2+} · L^{-1} ranged from 0.42 to 1.07 under PAR, from 0.42 to 0.98 under PA, and from 0.40 to 0.74 under PAB. Overall, the impact of UVA and UVB on growth was smaller when Zn^{2+} in the medium was more abundant (Fig. 2D).

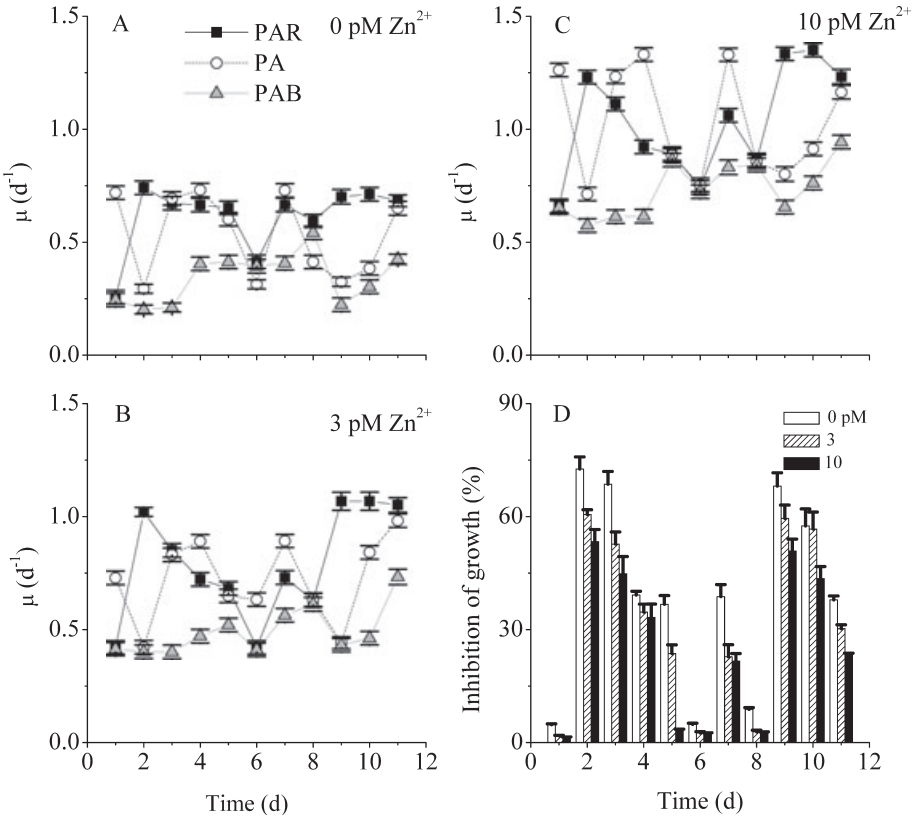

FIG. 2. Specific growth rate (μ) of *Skeletonema costatum* cultured at 0 (A), 3 (B), 10 (C) pmol $Zn^{2+} \cdot L^{-1}$. In panel D, the relative inhibition of μ by UVR, at different Zn^{2+} concentrations, over the duration of the experiment, is reported. The error bars indicate the standard deviations ($n = 3$).

Relationship between daily dose and growth at different Zn^{2+} concentrations. When the cells were grown under PAR treatment, the specific growth rate increased almost linearly with the increase in daily PAR dose in the presence of 3 ($R^2 = 0.89$, $P < 0.01$) or 10 ($R^2 = 0.82$, $P < 0.01$) pmol $Zn^{2+} \cdot L^{-1}$ (Fig. 3A). The only obvious deviation from linearity was observed on the first day of solar exposure after transfer from the growth cabinet to the outdoor (Fig. 3A, arrow). When the cells were cultured under PAR in the absence of Zn, no relevant change in growth rate was observed above 4.62 MJ $\cdot$ m^{-2} (Fig. 3A). Under the PA treatment (Fig. 3B), at all Zn^{2+} concentrations, μ increased when the daily dose increased from 3.44 to 5.09 MJ $\cdot$ m^{-2} ($P < 0.05$), remained stable within a dose range of 5.09 to 7.35 MJ $\cdot$ m^{-2}, and decreased when the dose exceeded 7.35 MJ $\cdot$ m^{-2} ($P < 0.05$). When the cultures were grown under PAB (Fig. 3C), μ increased with the dose from 3.45 to 4.95 MJ $\cdot$ m^{-2} ($P < 0.05$) and decreased from 5.02 to 5.45 MJ $\cdot$ m^{-2} ($P < 0.05$). From 5.71 MJ $\cdot$ m^{-2} to 6.56 MJ $\cdot$ m^{-2}, μ remained unaffected (0 pmol $Zn^{2+} \cdot L^{-1}$) or stimulated (3 and 10 pmol $Zn^{2+} \cdot L^{-1}$) by an increase in PAB dose ($P < 0.05$). From this dose upward, specific growth rates declined almost linearly. It is interesting that the highest μ values were recorded on the last day of experiments (6.56 MJ $\cdot$ m^{-2}) at 3 and 10 pmol $Zn^{2+} \cdot L^{-1}$) L^{-1}. This finding is suggestive of an acclimation of the cells to UVR and of a role of

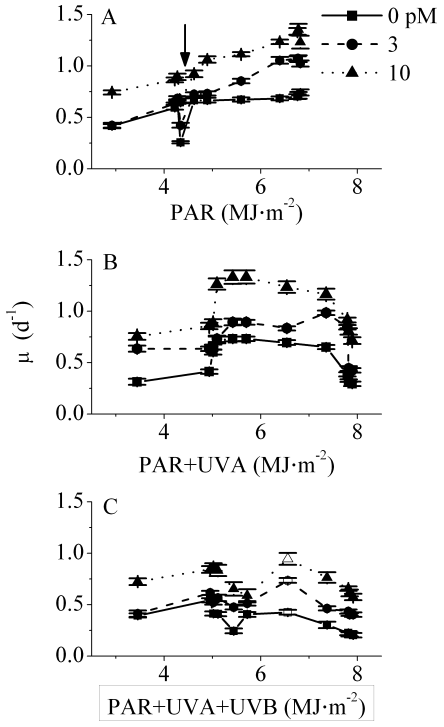

FIG. 3. Relationship between the specific growth rate (μ) of *Skeletonema costatum* grown at different Zn^{2+} concentrations and daily solar dose of PAR, PAR + UVA, and PAR + UVA + UVB. The arrows indicate the values measured on the first day of exposure, and the open symbols represent the value measured on the last day of exposure. The error bars indicate the standard deviations ($n = 3$).

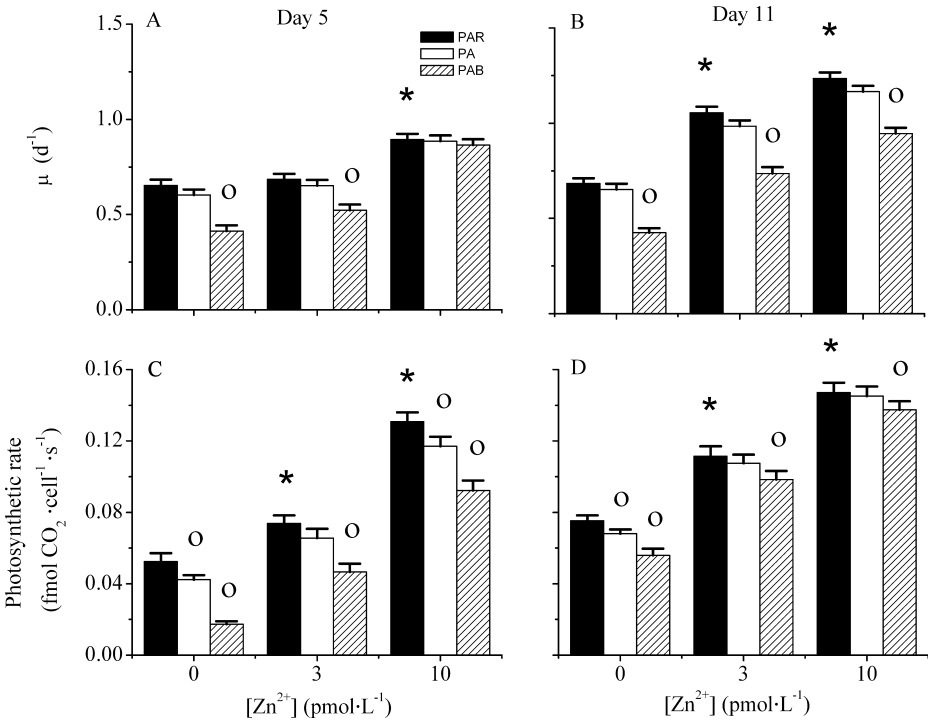

FIG. 4. Specific growth rate (A, B) and photosynthetic CO_2 assimilation rate (C, D) on the 5th and 11th days of exposure. The average solar irradiances on days 5 and 11 were 91.93 and 219.1 W · m^{-2} for PAR, 15.35 and 31.81 W · m^{-2} for UVA, and 0.29 and 0.72 W · m^{-2} for UVB. The solar daily dose on days 5 and 11, respectively, was 4.27 and 6.39 MJ · m^{-2} for PAR, 0.74 and 0.96 MJ · m^{-2} for UVA, and 0.018 and 0.021 MJ · m^{-2} for UVB. Circles indicate significant ($P < 0.05$) differences between different radiation treatment, and asterisks represent significant differences ($P < 0.05$) between different Zn^{2+} treatments. The error bars indicate the standard deviations ($n = 3$).

Zn^{2+} availability (see below). In general, enrichment of Zn^{2+} enhanced growth at all radiation treatments.

Effect of exposure time to PAR, UVA, UVB on growth. To observe if there is a time-dependent effect of Zn^{2+} concentration and solar radiation, we compared growth rates at different radiation treatments and Zn^{2+} concentrations on day 5 (Fig. 4A) and day 11 (Fig. 4B). On day 5, solar doses of PAR, UVA, and UVB were 4.27, 0.74, and 0.018 MJ · m^{-2}; on day 11, the doses were 6.39, 0.96, and 0.021 MJ · m^{-2}, for PAR, UVA, and UVB, respectively.

The specific growth rate was higher on day 11 than on day 5, regardless of the radiation and Zn^{2+} treatments, possibly as a consequence of the higher level of solar PAR on this day (Fig. 4, A and B). On day 5, no appreciable difference in μ was observed between 0 pmol $Zn^{2+} \cdot L^{-1}$ and 3 pmol $Zn^{2+} \cdot L^{-1}$ grown cultures. This trend was true for both the PAR and the PA treatments. A modestly higher growth rate was observed under PAB, when the cells were cultured at 3 pmol $Zn^{2+} \cdot L^{-1}$ rather than in the absence of Zn^{2+}. When the Zn^{2+} concentration in the culture medium was 10 pmol $\cdot L^{-1}$, growth rate under PAR increased by ~33% with respect to the other Zn^{2+} conditions. At this Zn^{2+} concentration, the presence of UVR did not affect growth (Fig. 4A). On day 5, the inhibition of growth by UVA was modest (1%–8%) and somewhat inversely dependent on Zn^{2+} concentration. UVB radiation inhibited growth at 0 and 3 pmol $Zn^{2+} \cdot L^{-1}$ (19%~29%), but had no appreciable effect at the highest Zn^{2+} concentration (Fig. 5A). On day 11, the effect of Zn^{2+} concentration was more obvious, and even a concentration of 3 pmol $\cdot L^{-1}$ caused a substantial increase in growth rate compared to the cultures with no Zn^{2+}. The increase in growth rate at higher Zn concentrations was observed for all radiation treatments on this day. The effect of UVR on growth at each Zn^{2+} concentration was more marked on day 11 than on day 5 (Fig. 5B), possibly because of the higher radiation dose on this day. The contribution of UVA to growth inhibition on day 11 is not related to the Zn^{2+} concentration and is rather modest (~6%–7%). Instead, UVB-dependent growth inhibition was substantial (19%–33%) and inversely related (although not linearly) with Zn availability (Fig. 5B).

Effect of the duration of the exposure to PAR, UVA, UVB on photosynthesis. Under the PAR treatment, the photosynthetic rates on day 5 (Fig. 4C) and day 11 (Fig. 4D) were respectively 41% and 48% higher at 3 pmol $\cdot L^{-1}$ Zn^{2+} and 149% and 95% higher at 10 pmol $\cdot L^{-1}$ Zn^{2+}, with respect to the cultures grown in the absence of Zn^{2+}. On day 5, the presence of UVA + UVB resulted in a significant decline in photosynthetic carbon fixation at all Zn^{2+} concentration (67% at 0, 37% at 3, and 29% at 10 pmol $Zn^{2+} \cdot L^{-1}$). On day 11, UVA + UVB had a smaller effect on photosynthesis, which declined by 26% at 0, 12% at 3 pmol $Zn^{2+} \cdot L^{-1}$, and did not vary significantly ($P > 0.05$) at 10 pmol $Zn^{2+} \cdot L^{-1}$. To separate the effect of UVA and UVB on photosynthesis, the percentage of inhibition caused by the PA treatment

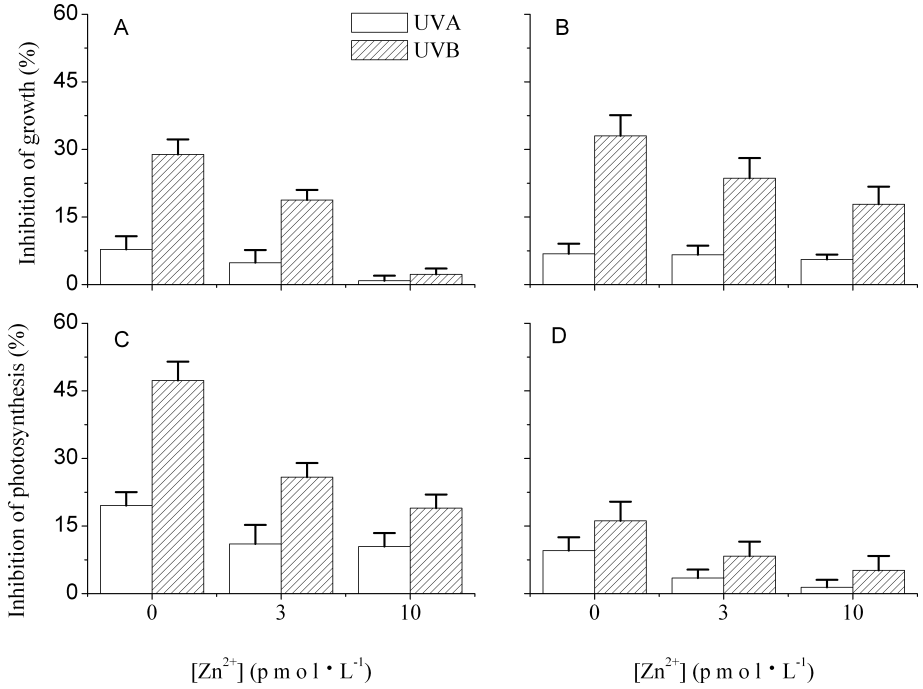

FIG. 5. Relative inhibition of specific growth rate (A, B) and photosynthetic CO_2 assimilation (C, D) by UVR on the 5th and 11th days of exposure. The error bars indicate the standard deviations ($n = 3$).

was subtracted from the percentage of inhibition caused by PAB (Fig. 5, C and D). These calculations showed unequivocally that UVB was the main effecter on photosynthesis on day 5 (19% to 47%), but its influence was greatly reduced on day 11 (5% to 16%). When UVB radiation was filtered out (PAR + UVA), the photosynthetic rate declined by 10% to 20% on day 5 and remained unaffected on day 11, with the only exception of the cells grown in the absence of Zn^{2+} (10% decrease). At any level of Zn^{2+}, UVB caused a much higher inhibition than UVA.

Effect of PAR, UVA, and/or UVB on the activity of eCA. Enrichment of Zn significantly promoted ($P < 0.05$) the activity of eCA both on day 4 and on day 10, regardless of the presence of UVR (Table 1). On day 4, UVR caused a reduction in the activity of eCA in cells grown at all Zn^{2+} concentration ($P < 0.05$). On day 10, the activity of eCA in cells cultured in the absence of Zn was still lower under PAB than under PAR ($P < 0.05$); however, at 3 pmol $Zn^{2+} \cdot L^{-1}$, UVR did not affect the activity of eCA ($P > 0.05$), and both UVA and UVA + UVB enhanced the activity of eCA ($P < 0.05$), when cells were cultured at 10 pmol $Zn^{2+} \cdot L^{-1}$. Interestingly, the rates of eCA activity were in large excess (three orders of magnitude) with respect to the photosynthetic rates. This was also true if other kinetic constants were used (data not shown).

The amount of enzymes per cell, calculated on the basis of the catalytic assumptions used for the rate estimates, was almost linearly dependent on Zn

TABLE 1. Catalytic rates of extracellular carbonic anhydrase (eCA) of *Skeletonema costatum* after 4 and 10 d of exposure to PAR (P), PAR + UVA (PA), or PAR + UVA + UVB (PAB).

		Day 4		Day 10	
$[Zn^{2+}]$ (pmol · L^{-1})	Radiation treatment	$\alpha_{CA}^{HCO_3^-}$ (fmol · cell^{-1} · s^{-1})	eCA content (fmol · cell^{-1})	$\alpha_{CA}^{HCO_3^-}$ (fmol · cell^{-1} · s^{-1})	eCA content (fmol · cell^{-1})
0	P	350.5 ± 29.51	0.020 ± 0.002	440.3 ± 30.02	0.025 ± 0.002
	PA	276.7 ± 29.39	0.016 ± 0.002	417.9 ± 28.80	0.024 ± 0.002
	PAB	219.2 ± 29.27	0.012 ± 0.002	383.2 ± 27.42	0.022 ± 0.002
3	P	767.7 ± 40.19	0.043 ± 0.002	1247 ± 34.18	0.070 ± 0.002
	PA	679.1 ± 35.88	0.038 ± 0.002	1210 ± 21.70	0.068 ± 0.001
	PAB	545.8 ± 60.07	0.031 ± 0.003	1218 ± 33.56	0.068 ± 0.002
10	P	1716 ± 84.15	0.096 ± 0.005	1682 ± 49.74	0.095 ± 0.003
	PA	1628 ± 31.39	0.092 ± 0.002	1832 ± 36.76	0.10 ± 0.002
	PAB	1567 ± 29.86	0.088 ± 0.002	1869 ± 37.79	0.11 ± 0.002

$\alpha_{CA}^{HCO_3^-}$, CA-catalyzed rates of HCO_3^- dehydration.
The values are the means ± D ($n = 3$).

availability and moderately dependent on the presence of UVR on day 4. On day 10, at 0 and 3 pmol $Zn^{2+} \cdot L^{-1}$, the amount of enzyme remained statistically unaffected by the radiation treatment and appeared to be strongly dependent on the concentration of Zn^{2+} in the growth medium. At the highest Zn^{2+} concentration, however, the abundance of eCA was higher when the cells were subjected to UVR.

Effect of the radiation treatments on chl a *and carotenoid cell content and on whole cell absorbtion spectra.* After 1 d of exposure to solar radiation, there was no significant difference in the content of chl *a* per cell between the PAR and the PAB treatments, at 3 and 10 pmol $Zn^{2+} \cdot L^{-1}$. However, at 0 pmol $Zn^{2+} \cdot L^{-1}$, the cell content of chl *a* under PAR was significantly lower than that under PA ($P < 0.05$) and significantly higher than that under PAB ($P < 0.05$) (Fig. 6, A–C). After 4 d of exposure to solar radiation, chl *a* declined in the presence of UVR regardless of the Zn^{2+} concentration. On day 11, at 10 pmol $Zn^{2+} \cdot L^{-1}$, the chl *a* content per cell under PAB was higher than that under PAR ($P < 0.05$). On the same day, however, at both 0 and 3 pmol $Zn^{2+} \cdot L^{-1}$, chl *a* per cell was still less abundant under PAB than under PAR. On days 4, 5, and 8, when the amount of radiation reaching the cultures was attenuated by clouds, the presence of UVR enhanced the carotenoid content per cell, at 3 pmol $Zn^{2+} \cdot L^{-1}$ and 10 pmol $Zn^{2+} \cdot L^{-1}$ ($P < 0.05$). On sunny days such as day 11, instead, the carotenoid content (Fig. 6, D–F) under PAB was lower than that under PAR in cells grown in media containing 0 pmol $Zn^{2+} \cdot L^{-1}$ and 10 pmol $Zn^{2+} \cdot L^{-1}$ ($P < 0.05$).

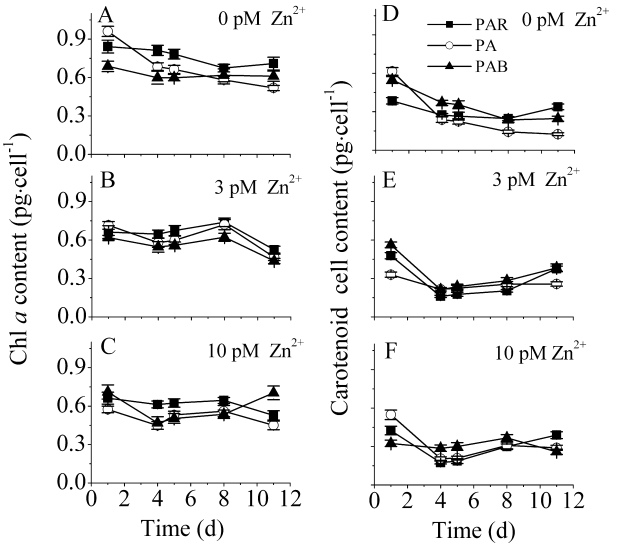

FIG. 6. Chl *a* and carotenoid content of *Skeletonema costatum* cells grown in the presence of different Zn^{2+} concentrations. The error bars indicate the standard deviations ($n = 3$). PA, PAR + UVA; PAB, PAR + UVA + UVB.

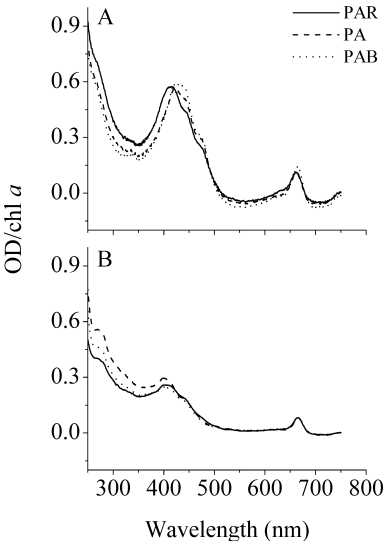

FIG. 7. Typical absorbance spectra of methanol extracts from *Skeletonema costatum* cells grown at 3 pmol $Zn^{2+} \cdot L^{-1}$ on the 5th (A) and 11th days (B) of exposure.

The absorbance spectra of cells sampled on day 5 and day 11 appeared somewhat different (Fig. 7). On day 5, the chl peaks were more prominent than on day 11, and this finding was also confirmed by the overall trends of the chl content (Fig. 6, A–C). On day 5, absorbance between 250 and 400 nm was somewhat reduced in the presence of UVR. The opposite could be observed for cells collected on day 11, where exposure to UVR appeared to have increased the absorbance in the spectral region 250 and 400 nm. Moreover, on day 11, a peak appears in the spectra ~270 nm. The integrated areas for the absorption peaks within the waveband (from 260 to 300 nm) under PAR, PA, and PAB were close to zero at day 5, but increased to 0.67 ± 0.07 under PAR, 1.03 ± 0.08 under PA, and 0.71 ± 0.06 under PAB at day 11, respectively. It was obvious that the cells had acclimated to screen off more UVB after a prolonged exposure (day 11).

DISCUSSION

The results reported in this paper show the following: (1) Growth and photosynthesis of *S. costatum*, under the growth conditions used for this study, were stimulated, under both PAR alone or PAB, by the increase of Zn^{2+} concentrations from 0 to 3 pmol $\cdot L^{-1}$ and from 3 to 10 pmol $\cdot L^{-1}$. (2) UVA effect on growth and photosynthesis was either stimulating or inhibitory depending on its dose and Zn availability, while UVB was always inhibitory. (3) UVR inhibition of growth and photosynthesis was lower at higher concentrations of Zn^{2+}. (4) Acclimation to UVR was accelerated when Zn^{2+} was more abundant.

The reasons for these observations may be numerous, and while more experiments may be required to obtain definitive answers, some conclusions can be derived.

Effect of Zn^{2+} concentration on growth and photosynthesis. Under the growth conditions used for this study, consistent with previous studies (Hu et al. 2003), Zn^{2+} was limiting at concentrations substantially higher than those commonly encountered in the ocean (Bruland 1989, Donat and Bruland 1990, Franck et al. 2003). However, the effect of Zn^{2+} deprivation in our cultures is likely to be strongly enhanced by the fact that the artificial medium used was enriched in a variety of micro- and macronutrients that, in oceanic seawater, could limit algal growth and primary production before Zn^{2+}.

In our cultures, Zn limitation seemed to be exerted at the level of photosynthesis and to have repercussions on the growth of *S. costatum*. The effect of Zn^{2+} on photosynthesis may be mediated by carbon acquisition (Hu et al. 2003). Specifically, Zn^{2+}availability may impact the expression (Lane and Morel 2000) and the activity of CA (Hu et al. 2003), which is commonly considered an important component of CCM (Giordano et al. 2005). CA activity and the estimated enzyme abundance of *S. costatum* are indeed substantially stimulated by an increase of Zn availability (Table 1), confirming that both the expression and the activity of this enzyme are highly sensitive to Zn availability. However, it remains to be clarified to what extent CA activity is related to the photosynthetic performance (and to growth), considering that CA catalytic rates were at all Zn^{2+} concentrations. This is not entirely surprising, since similar results had been observed for the green alga *Dunaliella salina* (Giordano and Bowes 1997), but it is nevertheless puzzling.

In this work, substantial growth was observed even when the cells were completely deprived of Zn^{2+}. This finding suggests that other metals can substitute for Zn with relatively high efficiency, in *S. costatum*, as already observed for other phytoplankton species (Morel et al. 1994, Sunda and Huntsman 1995, Xu et al. 2007). Internal reservoir of Zn may probably also explain the persistence of growth in a Zn-free medium. Since our cultures were aerated with ambient air, air-derived Zn^{2+} may have dissolved into the medium. However, even if this happened, such input would be modest and equal for the media with different Zn^{2+} concentrations.

Effect of UV radiation on growth and photosynthesis. It is interesting that, when the UVB was filtered out, PA either stimulated or inhibited growth in comparison with PAR alone, depending on the mean daily dose. On the cloudy days (low dose), in the presence of Zn^{2+}, the PA treatment generally afforded higher growth rates than PAR alone, while it inhibited growth on the sunny days (high dose; Fig. 2, B and C). Long wavelength UVA has been determined to drive photosynthetic O_2 evolution in algae (Neori et al. 1988), probably due to the extended absorption tail of chl *a* (Jeffrey et al. 1997). Direct evidence for UVA driven photosynthesis in the absence of PAR radiation was also recently reported in coastal phytoplankton assemblages by Gao et al. (2007). Other positive effects of UVA, such as the enhancement of repair of UVB damaged DNA (Buma et al. 2003), may have concurred to the stimulatory effect of UVA at low doses.

In the present study, regardless of the time of exposure to radiations and of the Zn^{2+} concentration, UVB almost invariably exerted an inhibitory effect on both photosynthesis and growth; although the total energy of UVA was generally much higher (44-fold, on average, during the experiment) than that of UVB, the largest percentages of inhibition was due to UVB because of its much higher energy per quantum (Fig. 5), as also observed for another marine diatom and a dinoflagellate (Cullen et al. 1992). The inhibitory effect of UVB was largely expected, since UVB is known to damage D1 protein (Sass et al. 1997) and DNA molecules (Buma et al. 2003), and affect nutrient uptake (Fauchot et al. 2000) and many other pivotal biological processes (Heraud and Beardall 2000, Liang et al. 2006).

Effect of Zn^{2+} on the responses to UVR. The sensitivity of cultures to UVR appeared to be related to the Zn concentration in the growth medium. The reason for this relationship may be associated with a general stimulation of photosynthesis due to the presence of Zn enzymes in the photosynthetic pathway or by the increased effectiveness of the CO_2-concentrating mechanisms caused by the increased CA abundance and activity. In addition, Zn-involved superoxide dismutase (SOD), the activity of which is closely related to Zn availability (Pandey et al. 2002), might have played a role in scavenging reactive oxygen species (ROS) induced by UVB (Mackerness et al. 2001). Therefore, activity of Zn-compounded SOD could have been stimulated to counteract the ROS-related damages. Zn could also play an important role in DNA repair, since many endonucleases contain Zn fingers (Kovalsky and Grossman 1994).

A possible direct role of Zn as a UV screen can also be hypothesized. Zn oxide (ZnO) is in fact well known to provide good protection from broadband UVR (Mitchnick et al. 1999). Such compound would not be visible in our methanol extracts, but its presence would explain the UVR responses observed as a function of Zn^{2+} concentration. Moreover, there are reports on the fact that diatoms tend to accumulate most of their Zn on their surface and allow only a limited amount of Zn inside the cell (Florence and Stauber 1990). This distribution would further point toward a role of Zn compounds as a UV screen. Since little Zn is required for growth and it can be effectively substituted by other divalent cations, if necessary, and since high Zn

amounts have been reported to have toxic effects on many microalgae (Rijstenbil et al. 1994 and references therein), the ability of retaining Zn on the cell surface may constitute an effective UV protective strategy for phytoplankton. Further investigations are required to identify the exact molecules involved.

If Zn exerts its protective action via these protective mechanisms, regardless of the precise mechanism, growth at low (i.e., present) CO_2, determining a diversion of Zn to highly inducible carbonic anhydrase, may increase sensitivity to UVR for cells with active CCMs, at suboptimal Zn^{2+} concentrations, as was observed by Sobrino et al. (2005) in *Nannochloropsis gaditana*. The stimulation of CA activity and the abundance and decreased sensitivity of growth and photosynthesis to UVR in *S. costatum* may thus be two concomitant but independent processes.

Acclimation. There was a sharp drop in the growth rate on the first day of solar exposure when the cells were transferred from the indoor (growth cabinet) to the outdoor (Fig. 3A, arrow) conditions. Such a decrease was caused by the irradiation shock. It was recently reported that the growth rate of the indoor-grown *S. costatum* equaled that of the seawater-isolated (wildtype) strain of the same species in ~2 d when they were grown under solar radiation in the presence of UVR simultaneously (Guan and Gao 2008). Considering the data collected over the last 3 d of the experiment, which had a similar daily dose, it can be observed that growth inhibition by UVA and UVB declines over time (Fig. 2). While it is difficult to ascertain whether acclimation processes took place over the entire duration of the experiment, due to the variability of daily dose, this portion of the temporal sequence provides convincing evidence for an acclimatory response.

A similar conclusion can be drawn for photosynthesis, comparing the CO_2-fixation rates on a day in the middle and on a day at the end of the radiation treatment: on day 5, in spite of a lower dose, inhibition of photosynthesis is appreciably higher than that observed on day 11 (Figs. 4 and 5). This trend is also true for the estimated catalytic rates of eCA (Table 1).

The same trend cannot be observed when the growth rates on days 5 and 11 are compared. This finding is indicative of an uncoupling of photosynthesis and growth, and of a greater sensitivity of growth to the daily UVR dose compared with photosynthesis. These changes could be the consequence of the often observed effect of UVR on the cell cycle, which induces the interruption of the cycle in the G2 phase, determining an increase in cell size but a reduction in division rates (Karentz et al. 1991, Buma et al. 1996).

It is worthwhile to observe that, especially after a prolonged exposure to UVR (day 11), the absorption in the UV regions seemed to increase slightly, but appreciably ($P < 0.05$) (Fig. 7B). This increase may be an indication that a modest capacity to screen UV was induced, thereby reducing the damaging impact of radiation, which accounts for the acclimation. A small peak in the UVB region was also observed in the absorption spectra of samples collected near the end of the experiment. A similar absorption band is given by phlorotannins, which were shown to protect marine brown algae from UVB (Pavia et al. 1997, Swanson and Druehl 2002).

In the dynamically changing environments of the ocean, Zn^{2+} concentration varies from area to area (Ellwood and Van den Berg 2000), while solar UV irradiances change with depth. Phytoplankton cells in seawater are usually tossed up and down with the movement of waves and mixing; changing levels of UVR during vertical mixing can reverse the effects of UVR from negative to positive (Helbling et al. 2003). Therefore, interactive or combined effects of Zn^{2+} and UVR can always be expected on the cells. The results reported here suggest that high levels of solar UVR may affect growth and photosynthesis of the diatom in surface waters, where Zn^{2+} is limiting and mixing is slow, while in waters where Zn^{2+} is abundant, moderate levels of UVA on cloudy days or under fast-mixing conditions may enhance the growth of this diatom.

This research was supported by National Natural Science Foundation of China (No. 90411018; No. 40573059) and Ministry of Education (No.308015).

Badger, M. R., Andrew, T. J., Whitney, S. M., Ludwig, M., Yellowlees, D. C., Leggat, W. & Price, G. D. 1998. The diversity and coevolution of Rubisco, plastids, pyrenoids, and chloroplast-based CO_2-concentrating mechanisms in algae. *Can. J. Bot.* 76:1052–71.

Barbieri, E. S., Villafañe, V. E. & Helbling, E. W. 2002. Experimental assessment of UV effects on temperate marine phytoplankton when exposed to variable radiation regimes. *Limnol. Oceanogr.* 47:1648–55.

Bischof, K., Kräbs, G., Wiencke, C. & Hanelt, D. 2002. Solar ultraviolet radiation affects the activity of ribulose-1,5-bisphosphate carboxylase-oxygenase and the composition of photosynthetic and xanthophyll cycle pigments in the intertidal green alga *Ulva lactuca* L. *Planta* 215:502–9.

Brand, L. E., Sunda, W. G. & Guillard, R. R. L. 1983. Limitation of marine-phytoplankton reproductive rates by zinc, manganese, and iron. *Limnol. Oceanogr.* 28:1182–98.

Bruland, K. W. 1989. Oceanic zinc speciation: complexation of zinc by natural organic ligands in the central North Pacific. *Limnol. Oceanogr.* 34:269–85.

Bruland, K. W., Donat, J. R. & Hutchins, D. A. 1991. Interactive influences of bioactive trace meals on biological production in oceanic waters. *Limnol. Oceanogr.* 36:1555–77.

Brunner, K. D., Zörb, C., Kolukisaoglu, H. Ü. & Wagner, G. 2000. Light-regulated transcription of a cryptochrome gene in the green alga *Mougeotia scalaris*. *Protoplasma* 214:194–8.

Buitenhuis, E. T., Timmermans, K. R. & de Baar, H. J. W. 2003. Zinc-bicarbonate colimitation of *Emiliania huxleyi*. *Limnol. Oceanogr.* 48:1575–82.

Buma, A. G. J., Boelen, P. & Jeffrey, W. H. 2003. UVR-induced DNA damage in aquatic organisms. *In* Helbling, E. W. & Zagarese, H. E. [Eds.] *UV Effects in Aquatic Organisms and*

Ecosystems. The Royal Society of Chemistry, Cambridge, UK, pp. 291–327.
Buma, A. G. J., Zemmelink, H. J., Sjollema, K. & Gieskes, W. W. C. 1996. UVB radiation modifies protein and photosynthetic pigment content, volume and ultrastructure of marine diatoms. *Mar. Ecol. Prog. Ser.* 142:47–54.
Chen, X. & Gao, K. 2003. Effect of CO_2 concentrations on the activity of photosynthetic CO_2 fixation and extracelluar carbonic anhydrase in the marine diatom *Skeletonema costatum*. *Chin. Sci. Bull.* 48:2616–20.
Chen, X. & Gao, K. 2004. Roles of carbonic anhydrase in photosynthesis of *Skeletonema costatum*. *J. Plant Physiol. Mol. Biol.* 30:511–16.
Cullen, J. J., Neale, P. J. & Lesser, M. P. 1992. Biological weighting function for the inhibition of phytoplankton photosynthesis by ultraviolet radiation. *Science* 258:646–50.
Donat, J. R. & Bruland, K. W. 1990. A comparison of two voltammetric techniques for determining zinc speciation in northeast Pacific Ocean waters. *Mar. Chem.* 28:301–23.
Ellwood, M. J. & Van den Berg, C. M. J. 2000. Zinc speciation in the northeastern Atlantic Ocean. *Mar. Chem.* 68:295–306.
Fauchot, J., Gosselin, M., Levasseur, M., Mostajir, B., Belzile, C., Demers, S., Roy, S. & Villegas, P. Z. 2000. Influence of UVB radiation on nitrogen utilization by a natural assemblage of phytoplankton. *J. Phycol.* 36:484–96.
Florence, T. M. & Stauber, J. L. 1990. Mechanism of toxicity of zinc to the marine diatom *Nitzschia closterium*. *Mar. Biol.* 105:519–24.
Franck, V. M., Bruland, K. W., Hutchins, D. A. & Brzezinski, M. A. 2003. Iron and zinc effects on silicic acid and nitrate uptake kinetics in three high-nutrient, low-chlorophyll (HNLC) regions. *Mar. Ecol. Prog. Ser.* 252:15–33.
Gao, K., Wu, Y., Li, G., Wu, H., Villafañe, V. E. & Helbling, E. W. 2007. Solar UV radiation drives CO_2 fixation in marine phytoplankton: a double-edged sword. *Plant Physiol.* 144:1–6.
Giordano, M., Beardall, J. & Raven, J. A. 2005. CO_2 concentrating mechanisms in algae: mechanisms, environmental modulation, and evolution. *Annu. Rev. Plant Biol.* 56:99–131.
Giordano, M. & Bowes, G. 1997. Gas exchange and C allocation in *Dunaliella salina* cells in response to the N source and CO_2 concentration used for growth. *Plant Physiol.* 15:1049–56.
Guan, W. & Gao, K. 2008. Light histories influence the impacts of solar ultraviolet radiation on photosynthesis and growth in a marine diatom, *Skeletonema costatum*. *J. Photochem. Photobiol. B Biol.* 91:151–6.
Häder, D. P., Lebert, M., Marangoni, R. & Colombetti, G. 1999. ELDONET: European Light Dosimeter Network hardware and software. *J. Photochem. Photobiol. B* 52:51–8.
Harrison, P. J., Waters, R. E. & Taylor, F. J. R. 1980. A broad spectrum artificial seawater medium for coastal and open ocean phytoplankton. *J. Phycol.* 16:28–35.
Helbling, E. W., Gao, K., Gonçalves, R. J., Wu, H. & Villafañe, V. E. 2003. Impact of natural ultraviolet radiation on rates of photosynthesis and on specific marine phytoplankton species. *Mar. Ecol. Prog. Ser.* 259:59–66.
Heraud, P. & Beardall, J. 2000. Changes in chlorophyll fluorescence during exposure of *Dunaliella tertiolecta* to UV radiation indicate a dynamic interaction between damage and repair processes. *Photosynth. Res.* 63:123–34.
Holm-Hansen, O. & Helbling, E. W. 1995. Técnicas para la medición de la productividad primaria en el fitoplancton. *In* Alveal, K., Ferrario, M. E., Oliveira, E. C. & Sar, E. [Eds.] *Manual de Métodos Ficológicos*. Universidad de Concepción, Concepción, Chile, pp. 329–50.
Hu, H., Shi, Y., Cong, W. & Cai, Z. 2003. Growth and photosynthesis limitation of marine red tide alga *Skeletonema costatum* by low concentrations of Zn^{2+}. *Biotechnol. Lett.* 25:1881–5.
Huang, K., Kunkel, T. & Beck, C. F. 2004. Localization of the blue-light receptor phototropin to the flagella of the green alga *Chlamydomonas reinhardtii*. *Mol. Cell. Biol.* 15:3605–14.
Jeffrey, S. W., Mantoura, R. F. C. & Bjornland, T. 1997. Data for the identification of 47 key phytoplankton pigments. *In* Jefrrey, S. W., Mantoura, R. F. C. & Wright, S. W. [Eds.] *Phytoplankton Pigments in Oceanographic Methodology*. UNESCO, Paris, pp. 661.
Karentz, D., Cleaver, J. E. & Mitchell, D. L. 1991. Cell survival characteristics and molecular responses of Antarctic phytoplankton to ultraviolet-B radiation. *J. Phycol.* 27:326–41.
Korbee-Peinado, N., Abdala-Díaz, R. T., Figueroa, F. L. & Helbling, E. W. 2004. Ammonium and UV radiation stimulate the accumulation of mycosporine-like amino acids in *Porphyra columbina* (Rhodophyta) from Patagonia, Argentina. *J. Phycol.* 40:248–59.
Kovalsky, O. I. & Grossman, L. 1994. The use of monoclonal antibodies for studying intermediates in DNA repair by the *Escherichia coli* Uvr(A)BC endonuclease. *J. Biol. Chem.* 269:27421–6.
Lane, T. W. & Morel, F. M. M. 2000. Regulation of carbonic anhydrase expression by zinc, cobalt, and carbon dioxide in the marine diatom *Thalassiosira weissflogii*. *Plant Physiol.* 123:345–52.
Liang, Y., Beardall, J. & Heraud, P. 2006. Effect of UV radiation on growth, chlorophyll fluorescence and fatty acid composition of *Phaeodactylum tricornutum* and *Chaetoceros muelleri* (Bacillariophyceae). *Phycologia* 45:605–15.
Lin, C. 2002. Blue light receptors and signal transduction. *Plant Cell* 14:S207–25.
Mackerness, S. A. H., John, C. F., Jordan, B. & Thomas, B. 2001. Early signaling components in ultraviolet-B responses: distinct roles for different reactive oxygen species and nitric oxide. *FEBS Lett.* 489:237–42.
Mitchnick, M. A., Fairhurst, D. & Pinnell, S. R. 1999. Microfine zinc oxide (Z-cote) as a photostable UVA/UVB sunblock agent. *J. Am. Acad. Dermatol.* 40:85–90.
Morel, F. M. M., Reinfelder, J. R., Roberts, S. B., Chamberlain, C. P., Lee, J. G. & Yee, D. 1994. Zinc and carbon co-limitation of marine phytoplankton. *Nature* 369:740–2.
Nelson, D. M., Trégure, P., Brezinski, M. A., Leynaert, A. & Quéguiner, B. 1995. Production and dissolution of biogenic silica in the ocean: regional dam and relationship to biogenic sedimentation. *Glob. Biogeochem. Cycles* 9:359–72.
Neori, A., Vernet, M., Holm-Hansen, O. & Haxo, F. T. 1988. Comparison of chlorophyll far-red and red fluorescence excitation spectra with photosynthetic oxygen action spectra for photosystem II in algae. *Mar. Ecol. Prog. Ser.* 44:297–302.
Nilawati, J. B., Greenberg, B. M. & Smith, R. E. H. 1997. Influence of ultraviolet radiation on growth and photosynthesis of two cold ocean diatoms. *J. Phycol.* 33:215–24.
Nimer, N. A., Warren, M. & Merrett, M. J. 1998. The regulation of photosynthetic rate and activation of extracellular carbonic anhydrase under CO_2-limiting conditions in the marine diatom *Skeletonema costatum*. *Plant Cell Environ.* 21:805–12.
Pandey, N., Pathak, G. C., Singh, A. K. & Sharma, C. P. 2002. Enzymic changes in response to zinc nutrition. *J. Plant Physiol.* 15:1151–3.
Parsons, T. R. & Strickland, J. D. H. 1963. Discussion of spectrophotometric determination of marine plant pigments, with revised equation for ascertaining chlorophylls and carotenoids. *J. Mar. Res.* 21:155–63.
Pavia, H., Cervin, G., Lindgren, A. & Åberg, P. 1997. Effects of UVB radiation and simulated herbivory on phlorotannins in the brown alga *Ascophyllum nodosum*. *Mar. Ecol. Prog. Ser.* 157:139–46.
Porra, R. J. 2002. The chequered history of the development and use of simultaneous equations for the accurate determination of chlorophylls a and b. *Photosynth. Res.* 73:149–56.
Ratti, S., Morse, D. & Giordano, M. 2007. CO_2 concentrating mechanisms of the potentially toxic dinoflagellate *Protoceratium reticulatum* (Dinophyceae, Gonyaulacales). *J. Phycol.* 43:693–701.
Raven, J. A. & Beardall, J. 2003. Carbon acquisition mechanisms in algae: carbon dioxide diffusion and carbon dioxide concentrating mechanisms. *In* Larkum, A. W. D., Douglas, S. E. & Raven, J. A. [Eds.] *Photosynthesis in Algae*. Kluwer, Dordrecht, the Netherlands, pp. 225–44.

Raven, J. A. & Falkowski, P. G. 1999. Oceanic sinks for atmospheric CO_2. *Plant Cell Environ.* 22:741–55.

Rijstenbil, J. W., Derksen, J. W. M., Gerringa, L. J. A., Poortvliet, T. C. W., Sandee, A., van den Berg, M., van Drie, J. & Wijnholds, J. A. 1994. Oxidative stress induced by copper: defense and damage in the marine planktonic diatom *Ditylum brightwellii*, grown in continuous cultures with high and low zinc levels. *Mar. Biol.* 119:583–90.

Rost, B., Riebesell, U. & Sultemeyer, D. 2006. Carbon acquisition of marine phytoplankton: effect of photoperiod length. *Limnol. Oceanogr.* 51:12–20.

Sanyal, G. & Maren, T. H. 1981. Thermodynamics of carbonic anhydrase catalysis. *J. Biol. Chem.* 256:608–12.

Sass, L., Spetea, C., Máté, Z., Nagy, F. & Vass, I. 1997. Repair of UVB induced damage of photosystem II via de novo synthesis of the D1 and D2 reaction centre subunits of *Scynechocystis* sp. PCC 6803. *Photosynth. Res.* 54:55–62.

Schofield, O., Kroon, B. M. A. & Prezelin, B. B. 1995. Impact of ultraviolet radiation on photosystem II activity and its relationship to the inhibition of carbon fixation rates for Antarctic ice algae communities. *J. Phycol.* 31:242–8.

Shi, Y., Hu, H., Ma, R., Cong, W. & Cai, Z. 2004. Improved use of organic phosphate by *Skeletonema costatum* through regulation of Zn^{2+} concentrations. *Biotechnol. Lett.* 26:747–51.

Sobrino, C., Neale, P. J. & Lubián, L. M. 2005. Interaction of UV radiation and inorganic carbon supply in the inhibition of photosynthesis: spectral and temporal responses of two marine picoplankters. *Photochem. Photobiol.* 81:384–93.

Sunda, W. G. & Huntsman, S. A. 1992. Feedback interaction between zinc and phytoplankton in seawater. *Limnol. Oceanogr.* 37:25–40.

Sunda, W. G. & Huntsman, S. A. 1995. Cobalt and zinc interreplacement in phytoplankton: biological and geochemical implications. *Limnol. Oceanogr.* 40:1404–17.

Swanson, A. K. & Druehl, L. D. 2002. Induction, exudation and the UV protective role of kelp phlorotannins. *Aquat. Bot.* 73:241–53.

Tobin, A. J. 1970. Carbonic anhydrase from parsley leaves. *J. Biol. Chem.* 245:2656–66.

Vallee, B. L. & Auld, D. S. 1990. Zinc coordination, function and structure of zinc enzymes and other proteins. *Biochemistry* 29:5647–59.

Villafañe, V. E., Sundbäck, K., Figueroa, F. L. & Helbling, E. W. 2003. Photosynthesis in the aquatic environment as affected by UVR. *In* Helbling, E. W. & Zagarese, H. E. [Eds.] *UV Effects in Aquatic Organisms and Ecosystems.* Royal Society of Chemistry, Cambridge, UK, pp. 357–98.

West, L. J. A., Greenberg, B. M. & Smith, R. E. H. 1999. Ultraviolet radiation effects on a microscopic green alga and the protective effects of natural dissolved organic matter. *Photochem. Photobiol.* 69:536–44.

Wilbur, K. M. & Anderson, N. G. 1948. Electrometric and colorimetric determination of carbonic anhydrase. *J. Biol. Chem.* 176:147–54.

Xenopoulos, M. A., Frost, P. C. & Elser, J. J. 2002. Joint effects of UV radiation and phosphorus supply on algal growth rate and elemental composition. *Ecology* 83:423–35.

Xu, Y., Dang, T., Shaked, Y. & Morel, F. M. M. 2007. Zinc, cadmium, and cobalt interreplacement and relative use efficiencies in the coccolithophore *Emiliania huxleyi*. *Limnol. Oceanogr.* 52:2294–305.